

12-2008

# Electrodeposition of Nickel Nanowires and Nanotubes Using Various Templates

Asli Ertan

Cleveland State University, aslican76@yahoo.com

Surendra N. Tewari

Cleveland State University, s.tewari@csuohio.edu

Orhan Talu

Cleveland State University, o.talu@csuohio.edu

Follow this and additional works at: [https://engagedscholarship.csuohio.edu/encbe\\_facpub](https://engagedscholarship.csuohio.edu/encbe_facpub)

 Part of the [Materials Science and Engineering Commons](#), [Membrane Science Commons](#), and the [Nanoscience and Nanotechnology Commons](#)

**How does access to this work benefit you? Let us know!**

## *Publisher's Statement*

This is an Author's Accepted Manuscript of an article published in Journal of Experimental Nanoscience December 2008, available online: <http://www.tandfonline.com/10.1080/17458080802570617>

## Original Citation

Ertan, A., Tewari, S. N., & Talu, O. (2008). Electrodeposition of nickel nanowires and nanotubes using various templates. *Journal Of Experimental Nanoscience*, 3(4), 287-295. doi:10.1080/17458080802570617

## Repository Citation

Ertan, Asli; Tewari, Surendra N.; and Talu, Orhan, "Electrodeposition of Nickel Nanowires and Nanotubes Using Various Templates" (2008). *Chemical & Biomedical Engineering Faculty Publications*. 39.

[https://engagedscholarship.csuohio.edu/encbe\\_facpub/39](https://engagedscholarship.csuohio.edu/encbe_facpub/39)

This Article is brought to you for free and open access by the Chemical & Biomedical Engineering Department at EngagedScholarship@CSU. It has been accepted for inclusion in Chemical & Biomedical Engineering Faculty Publications by an authorized administrator of EngagedScholarship@CSU. For more information, please contact [library.es@csuohio.edu](mailto:library.es@csuohio.edu).

# Electrodeposition of nickel nanowires and nanotubes using various templates

Asli Ertan\*, Surendra N. Tewari and Orhan Talu

*Department of Chemical and Biomedical Engineering, Cleveland State University, Cleveland, OH, USA*

Nickel nanotubes and nanowires are grown by galvanostatic electrodeposition in the pores of 1000, 100, and 15 nm polycarbonate as well as in anodised alumina membranes at a current density of  $10 \text{ mA cm}^{-2}$ . The effects of pore size, porosity, electrodeposition time, effective current density, and pore aspect ratio are investigated. Nickel nanotube structures are obtained with 1000 nm pore size polycarbonate membrane without any prior treatment method. At the early stages of electrodeposition hollow nickel nanotubes are produced and nanotubes turn into nanowires at longer depositon times. As effective current density accounting for the membrane porosity decreases, the axial growth direction is favoured yielding nanowires rather than nanotubes. However, for smaller pore size polycarbonate membranes, nanowires are obtained even though effective current densities were higher. We believe that when the pore diameter is below a critical size, nanowires grow regardless of current density since narrow pores promote layer by layer growth of nanorods due to smaller surface area of the pore bottom compared to pore walls. Pore size has a dominant effect over effective current density in determining the structure of the fibres produced for small pores. Nickel nanowires are also obtained in the small pores of anodised alumina, which has higher aspect ratios. High aspect ratio membranes favour the fabrication of nanowires regardless of current density.

**Keywords:** nickel; nanotube; nanowire; electrodeposition

## 1. Introduction

Fabrication of nanowire arrays has recently attracted significant attention due to their important potential applications such as optical and magnetic media, sensors, electronic devices, catalysis, etc. [1–7]. Several studies have been performed to produce metal nanowires in templates since the size and the shape of the nanowires can be controlled easily and accurately [8]. Hollow tubular nanostructures have been investigated extensively because of their projected use in drug delivery, catalysis, and chemical and biological separation applications [9]. Galvanic displacement reactions, chemical vapour

---

infiltration [8], and coating surfaces of colloidal particles [10] have been employed to prepare tubular nanostructures. In this work, nickel nanowires and nanotubes are fabricated by using template-assisted electrochemical deposition process. Electrochemical deposition is a promising technique for the fabrication of nanostructures in a bottom-up trend and it does not require the employment of complex instrumentation [11–14].

In this study, we have used commercial anodised alumina, lab-made anodised alumina, and track-etch polycarbonate membrane templates. Anodised alumina is a commonly used template [15,16]. Our lab has produced alumina membranes having uniform diameter and ordered fine structure, as compared with the commercially anodised alumina that contained disordered and noncontinuous pore channels. These membranes are fabricated by anodic oxidation of aluminum metal sheet. Polycarbonate membranes allow producing continuous and uniform nanowires but their pore density is significantly smaller than anodised alumina.

## 2. Experimental

Pore characteristics of templates used in this study are listed in Table 1, and their typical microstructures are shown in Figure 1. The polycarbonate membranes (Whatman Corp.) were sputter coated with about 30 nm thick gold layer on one side. The gold-coated side of the membrane was then placed on a copper sheet, which constitutes the cathode of the set-up. A few drops of water were added on the membrane to promote its adhesion to the copper sheet and care was exercised to prevent trapped air bubbles (Figure 2).

The electrolyte solution used for nickel electrodeposition was  $53.6 \text{ g L}^{-1}$  of  $\text{NiSO}_4 \cdot 6\text{H}_2\text{O}$  having  $30 \text{ g L}^{-1}$  of  $\text{H}_3\text{BO}_3$  as a stabiliser. The pH of the solution was around 4.6. Deionised water with  $18 \text{ M}\Omega$  resistivity was used to prepare the solutions. Galvanostatic electrodeposition was performed with a constant current density of  $10 \text{ mA cm}^{-2}$  (based on the total area of the cathode). In all cases, this current resulted in a corresponding potential of 2–3 V. All of the experiments were conducted at room temperature. Solartron 1280B electrochemical test system was used as the power source and data acquisition system for the electrodeposition. After deposition, the sample was washed thoroughly with deionised water. Dissolution of the polycarbonate support using dichloromethane ( $\text{Cl}_2\text{CH}_2$ ) revealed the morphology of the nanostructure growth in membrane protruding from the surface for easy imaging. Finally, the morphology of nickel nanostructures was characterised using optical microscope, scanning electron microscopy (SEM) and energy dispersive X-ray analysis (EDX).

The above described procedure was also used to grow nickel nanostructures in commercial and lab-made anodised alumina membranes, except for using gallium–indium coating to achieve conductance at the cathode instead of gold sputtering. Commercial alumina membrane (Whatman Corp.) has a pore size range of 80–200 nm with a nominal thickness of  $60 \mu\text{m}$ , whereas lab-made anodised alumina has a pore diameter of 60 nm with a nominal thickness of  $80 \mu\text{m}$ . The lab-made alumina membrane was produced by 40 V anodization in oxalic acid for 24 h [17,18]. Alumina membranes were partially dissolved using NaOH solution. The cross sections of the lab-made and commercial alumina membranes are presented in Figure 3.

Table 1. Pore characteristics of the templates used in this study and other studies.

Membranes	Pore size (nm)	Effective current density ( $\text{mA cm}^{-2}$ )	Pore density ( $\text{cm}^{-2}$ )	Thickness ( $\mu\text{m}$ )	Aspect ratio	Surface porosity (%)
Polycarbonate membrane (this study)	1000	63.7 (hollow)	$2 \times 10^7$	11	$\sim 11$	$\sim 15.7$
	100	417 (solid)	$3 \times 10^8$	6	$\sim 60$	$\sim 2.4$
	15	9091 (solid)	$6 \times 10^8$	6	$\sim 400$	$\sim 0.11$
Commercial alumina (this study)	80–200	26.7 (solid)	$1 \times 10^9$	60	$\sim 300$	$\sim 25\text{--}50$
Lab-made alumina (this study)	60	6.7 (solid)	$3 \times 10^{10}$	80	$\sim 1300$	$\sim 30$
Polycarbonate (from [2])	400	12 (solid), 800 (hollow) with agent	$1 \times 10^8$	6–10	$\sim 20$	$\sim 12.5$
Commercial alumina (from [4])	80–200	0.8 (hollow) with agent	$1 \times 10^9$	60	$\sim 300$	$\sim 25\text{--}50$
Commercial alumina (from [9])	80–200	0.35(hollow) with triblock copolymer	$1 \times 10^9$	60	$\sim 300$	$\sim 25\text{--}50$
Commercial alumina (from [1])	80–200	26.7 (solid)	$1 \times 10^9$	60	$\sim 300$	$\sim 25\text{--}50$

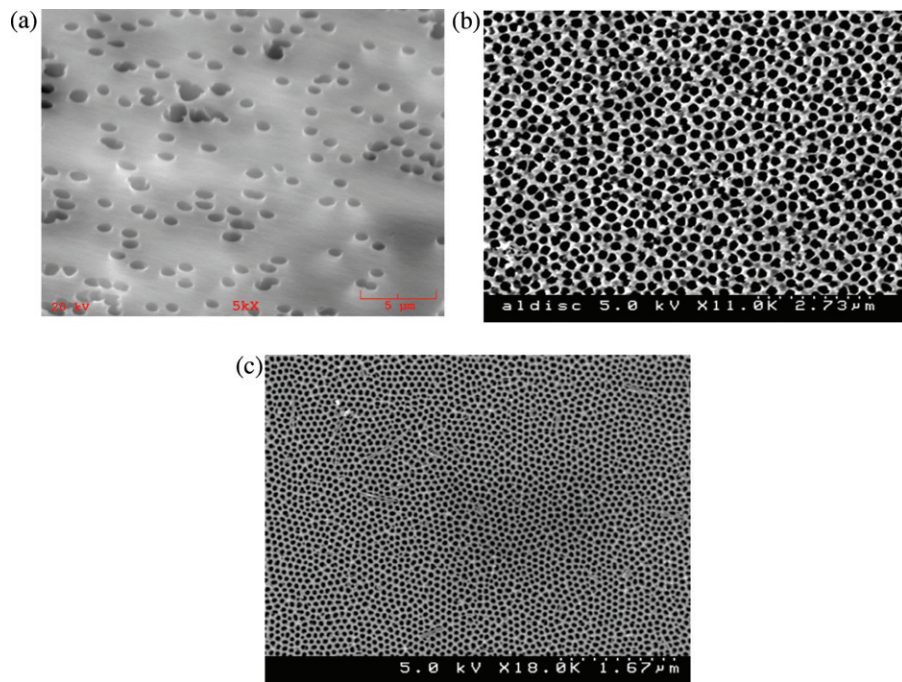


Figure 1. Bare membrane templates: (a) track-etch polycarbonate (b) commercial alumina (c) lab-made alumina.

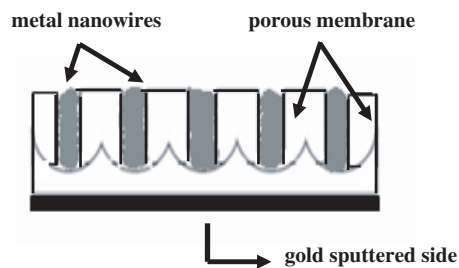


Figure 2. Schematic diagram of the procedure used to fabricate nickel nanowires.

### 3. Results and discussion

Previous studies suggest that nanotube growth is possible with a chemical modification of the inner surface of the pores prior to deposition [2,4]. In this study, nickel hollow tubes were grown in polycarbonate membranes with 1000 nm pore size applying a  $10 \text{ mA cm}^{-2}$  current density without any chemical modification. These samples are composed of well-defined nickel hollow nanotubes that are about  $2.5 \mu\text{m}$  long and have 1000 nm outer diameter and 200 nm inner diameter (Figure 4). Detailed examination of samples showed that deposition of nickel starts at the gold layer at the bottom circumference of the pores, and the nickel tubes grow along the pore wall through the top of the membrane.

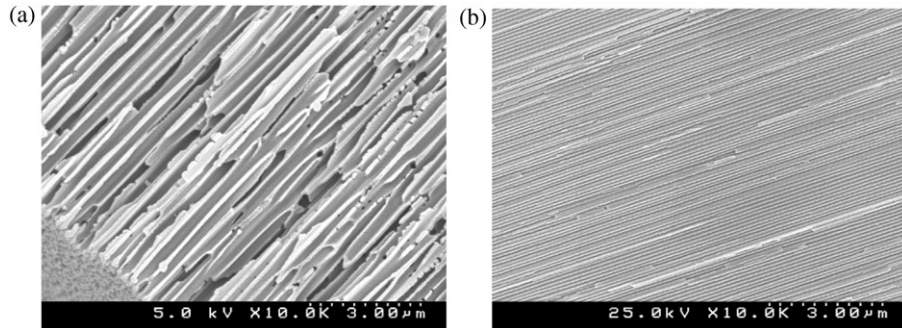


Figure 3. SEM micrographs showing the cross-sections of (a) commercial anodised alumina and (b) lab-made anodised alumina membrane at the same magnification.

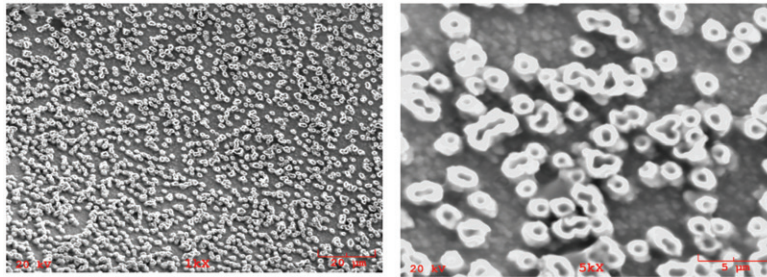


Figure 4. SEM micrographs showing nickel nanotubes deposited in 1000 nm polycarbonate membrane partially dissolved with dichloromethane.

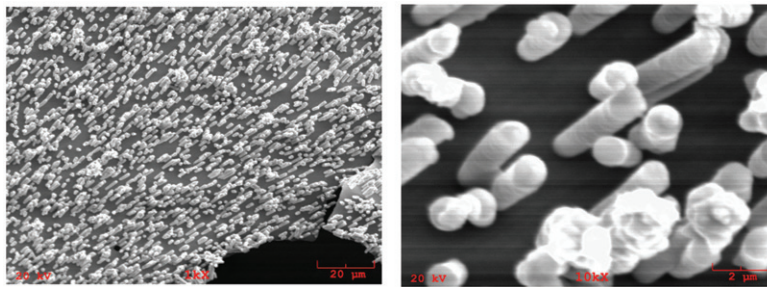


Figure 5. SEM micrographs showing nickel nanorods deposited in 1000 nm polycarbonate membrane dissolved with dichloromethane at a longer time.

Preferred deposition along the pore wall surface may be due to the large surface area available providing energetically favourable sites for the adsorption of the metal ions before being reduced [19]. These nanotubes were formed at early stages of the electrodeposition (Figure 4), corresponding to 30 min of deposition time. At longer electrodeposition times of around 35 min, the nanotubes turned into nanorods (Figure 5). Figures 4 and 5 also show that the metal deposition in the membranes are nearly

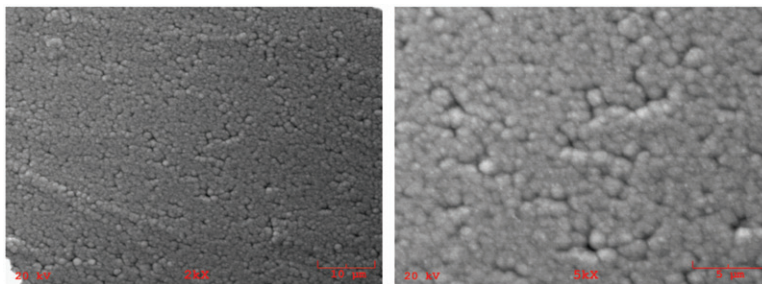


Figure 6. SEM micrographs showing nickel overgrowth on 1000 nm polycarbonate membrane.

perpendicular to the membrane surface, i.e., the heights of the fibres are constant indicating a uniform nickel growth in each pore of the membrane. Once the pores are completely filled with nickel, further electrodeposition produces hemispherical caps on the membrane surface, which subsequently merge together and result in a continuous overgrowth film (Figure 6).

Nickel fibre synthesis conditions for other studies are presented in Table 1 for comparison purposes. In order to eliminate the effect of nonconducting nonporous membrane area on current density, we calculated the effective current densities based on pore density and pore diameter. It is interesting to note that Xue et al. [2] obtained nanotubes in polycarbonate membranes by using pore-wall-modifying agents and increasing the voltage, and not by decreasing the deposition time (Table 1). They obtained nickel nanowires when  $12 \text{ mA cm}^{-2}$  effective current density was applied. The effective current density was increased to  $800 \text{ mA cm}^{-2}$  and wall-modifying agent was applied so that nucleation sites on the walls of the pores and nanotubes are produced. It was also shown by other groups that nickel nanotubes can be produced at very low-current densities as long as wall-modifying agents are being used [2,4] (Table 1). However, chemical modification of the inner walls of the template introduces impurities to the system [2].

Current density of  $10 \text{ mA cm}^{-2}$  was applied to smaller pore size polycarbonate membranes to see the effect of pore size, porosity and hence effective current density. Normally, hollow nanotubes have a tendency to grow in higher current densities. Slow growth with low-current density yield to solid nanorods [2,7,19]. As can be seen in Table 1, in the present study, the effective current density increases with decreasing pore size, which should normally result in nanotubes, not in nanorods. However, instead of nanotubes, we obtained solid rods for 100 and 15 nm polycarbonate membranes at high effective current densities (Figure 7). Due to this observation, we believe that the pore size has a dominant effect over effective current density in controlling the structure of the nanometals below a certain size. One other parameter that has an effect on the structures of the nanorods formed is the aspect ratio, which is defined as the length over diameter ratio. It has been reported in literature that high aspect ratio membranes favour the formation of nanowires [20, 21]. In our study, we obtained nanowires/nanorods for templates with aspect ratios of 60 and higher whereas hollow nanotubes were formed with a much lower aspect ratio which is 11. Although, preferential growth mechanism depends on effective current density we believe that under a critical pore size solid rods will be formed if high aspect ratio templates are used. Deep and narrow pores promote layer by layer growth of nanorods.

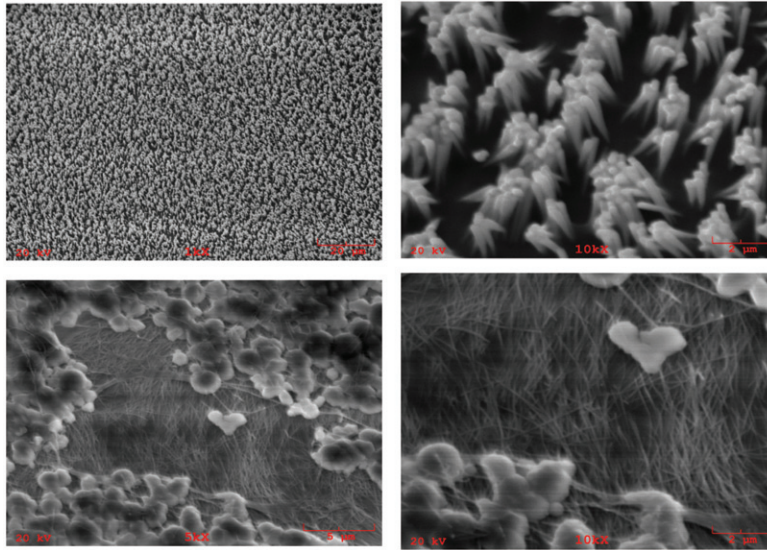


Figure 7. SEM micrographs showing nickel solid rods deposited in 100 nm (first row) and 15 nm (second row) polycarbonate membranes partially dissolved with dichloromethane.

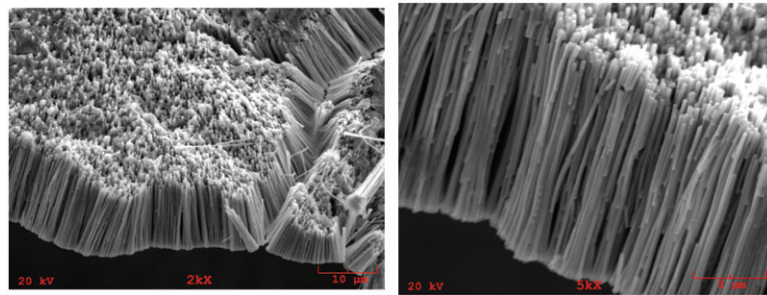


Figure 8. SEM micrographs showing nickel solid rods deposited in commercial alumina membrane. The metal array stays together even after complete dissolution of alumina membrane with NaOH solution.

In contrast in larger pore sizes, the metal can grow on the inner wall of the pores and form nanotubes. Thus, resulting structure is determined by an intricate interplay between pore size (through effective current density) and aspect ratio.

Same conditions were applied to our second group of membranes; anodised alumina. For both commercial and lab-made alumina membranes solid nanowires were obtained (Figures 8 and 9) supporting the above statements about aspect ratio and pore size. It has been reported that solid rods were obtained when applying the same conditions to commercial alumina membranes (Table 1) [1]. As can be seen from Figure 8, the nanorods were grown to same height and were uniformly produced in each pore of the membrane. The diameter of the nanorods obtained in commercial alumina is around 200 nm, whereas

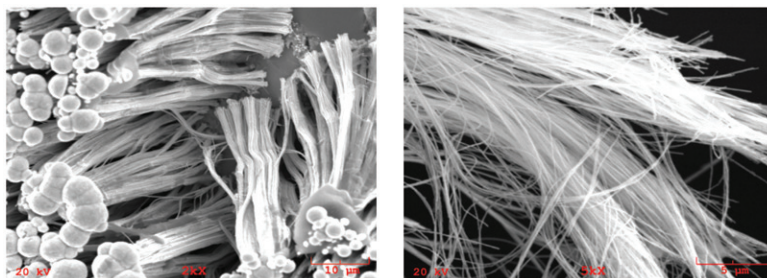


Figure 9. SEM micrographs showing nickel solid rods deposited on lab-made alumina membrane dissolved with NaOH solution. Overgrowth caps are visible on the left image.

much finer nickel fibres with 60 nm diameter were obtained for lab-made alumina, both determined by the pore size of the membranes. The density of these structures is orders of magnitude higher than polycarbonate grown nanorods in accordance with the much higher pore density of anodised alumina membranes. The density is so high that the metal array stays together even after the alumina template is completely dissolved.

It is not expected to grow nanotubes with anodised alumina membranes, which have high aspect ratio and high pore density (resulting in lower effective current densities). Both factors promote the growth of nanorods rather than nanotubes.

#### 4. Conclusions

The effects of pore size, porosity, deposition time, effective current density, and aspect ratio on the fabrication of nickel nanostructures were examined. Nickel nanotubes were obtained with 1000 nm pore size polycarbonate membranes without any chemical treatment of pore walls. As the deposition time increases, nanotubes turn into solid rods. As the porosity of the membrane increases, the effective current density decreases due to the larger exposed area. Lower porosity and hence higher current density favours the production of hollow nanostructures as was shown by 1000 nm polycarbonate membranes. However, we could not obtain hollow fibres with smaller size polycarbonate membranes and with anodised alumina templates even at high-current density. We believe that below a critical pore size, solid rods will be formed through layer by layer mechanism regardless of current density due to the smaller surface area of the pore bottom compared to pore walls. One last parameter that is considered is the aspect ratio. In our study, we obtained nanowires with aspect ratios of 60 and higher and nanotubes were formed at a much lower aspect ratio which is 11. Thus, we conclude that the morphology of nanostructures is a result of an intricate play between current density, pore size, and aspect ratio.

#### Acknowledgements

This work was supported by US Department of energy (contract# DE-FC 36-04ER14007). We thank to Mr Pradeep Kodumuri for his help in preparing the lab-made anodised alumina membrane.

## References

- [1] I.Z. Rahman, K.M. Razeeb, M. Kamruzzaman, and Md. Serantoni, *Characterisation of electrodeposited nickel nanowires using NCA template*, J. Mater. Process. Technol. 153–154 (2004), pp. 811–815.
- [2] S. Xue, C. Cao, and H. Zhu, *Electrochemically and template-synthesized nickel nanorod arrays and nanotubes*, J. Mater. Sci. 41 (2006), pp. 5598–5601.
- [3] K.R. Pirota, D. Navas, M.H. Velez, K. Nielsch, and M. Vazquez, *Novel magnetic materials prepared by electrodeposition techniques: Arrays of nanowires and multi-layered microwaves*, J. Alloys Compd. 369 (2004), pp. 18–26.
- [4] J. Bao, C. Tie, Z. Xu, Q. Zhou, D. Shen, and Q. Ma, *Template synthesis of an array of nickel nanotubules and its magnetic behavior*, Adv. Mater. 13 (2001), pp. 1631–1633.
- [5] M. Steinhart, Z. Jia, A.K. Schaper, R.B. Wehrspohn, U. Gosele, and H. Wendorff, *Palladium nanotubes with tailored morphologies*, Adv. Mater. 15 (2003), pp. 706–709.
- [6] H.Q. Cao, Y. Xu, J. Hong, H. Liu, G. Yin, B. Li, C. Tie, and Z. Xu, *Sol-gel template synthesis of an array of single crystal CdS nanowires on a porous alumina template*, Adv. Mater. 13 (2001), pp. 1393–1394.
- [7] R. Kaur, N.K. Verma, and S. Kumar, *Fabrication of copper microcylinders in polycarbonate membranes and their characterization*, J. Mater. Sci. 41 (2006), pp. 3723–3728.
- [8] B.K. Lee, S.M. Lee, and J. Cheon, *Size-controlled synthesis of Pd nanowires using a mesoporous silica template via chemical vapor infiltration*, Adv. Mater. 13 (2001), pp. 517–520.
- [9] F. Tao, M. Guan, Y. Jiang, J. Zhu, Z. Xu, and Z. Xue, *An easy way to construct an ordered array of nickel nanotubes: The triblock-copolymer-assisted hard-template method*, Adv. Mater. 18 (2006), pp. 2161–2164.
- [10] Y. Sun, B. Mayers, and Y. Xia, *Metal nanostructures with hollow interiors*, Adv. Mater. 15 (2003), pp. 641–646.
- [11] M. Zhang, S. Lenhart, M. Wang, L. Chi, H. Lu, and N. Ming, *Regular arrays of copper wires formed by template-assisted electrodeposition*, Adv. Mater. 16 (2004), pp. 409–413.
- [12] K. Nielsch, F. Muller, A.P. Li, and U. Gosele, *Uniform nickel deposition into ordered alumina pores by pulsed electrodeposition*, Adv. Mater. 12 (2000), pp. 582–586.
- [13] S. Pignard, G. Goglio, A. Radulescu, and L. Piroux, *Study of the magnetization reversal in individual nickel nanowires*, J. Appl. Phys. 87 (2000), pp. 824–829.
- [14] C. Schonenberger, B.M.I. Zande, L.G.J. Fokkink, M. Henny, C. Schmid, M. Kruger, A. Bachtold, R. Huber, H. Birk, and U. Staufer, *Template synthesis of nanowires in porous polycarbonate membranes: Electrochemistry and Morphology*, J. Phys. Chem. B. 101 (1997), pp. 5497–5505.
- [15] T. Yanagishita, M. Sasaki, K. Nishio, and H. Masuda, *Carbon nanotubes with a triangular cross-section, fabricated using anodic porous alumina as the template*, Adv. Mater. 16 (2004), pp. 429–432.
- [16] Y.T. Tian, G.W. Meng, T. Gao, S.H. Sun, T. Xie, X.S. Peng, C.H. Ye, and L.D. Zhang, *Alumina nanowire arrays standing on a porous anodic alumina membrane*, Nanotechnology 15 (2004), pp. 189–191.
- [17] L. Ba and W.S. Li, *Influence of anodizing conditions on the ordered pore formation in anodic alumina*, J. Phys. D: Appl. Phys. 33 (2000), pp. 2527–2531.
- [18] Y. Piao, H. Lim, J.Y. Chang, W.Y. Lee, and H. Kim, *Nanostructured materials prepared by use of ordered porous alumina membranes*, Electrochim. Acta 50 (2005), pp. 2997–3013.
- [19] H. Cao, L. Wang, Y. Qiu, G. Wang, L. Zhang, and X. Liu, *Generation and growth mechanism of metal (Fe, Co, Ni) nanotube arrays*, Chemphyschem 7 (2006), pp. 1500–1504.
- [20] Y. Liu, D. Ma, R.A. Blackley, W. Zhou, X. Han, and X. Bao, *Synthesis and characterization of Gibbsite nanostructures*, J. Phys. Chem. C. 112 (2008), pp. 4124–4128.
- [21] E.A. Vasconcelos, F.R.P. Santos, E.F. Silva, and H. Boudinov, *Nanowire growth on Si wafers by oxygen implantation and annealing*, Appl. Surf. Sci. 252 (2006), pp. 5572–5574.